UCLA
UCLA Previously Published Works

## Title

Electrochemiluminescence methods using CdS quantum dots in aptamer-based thrombin biosensors: a comparative study.

## Permalink

https://escholarship.org/uc/item/8p72p37x

## Journal

Mikrochimica acta, 187(1)

## ISSN

0026-3672

## Authors

Isildak, Ibrahim
Navaeipour, Farzaneh
Afsharan, Hadi
et al.

## Publication Date

2019-12-06

## DOI

10.1007/s00604-019-3882-y

Peer reviewed

eScholarship.org Powered by the California Digital Library
University of California

Microchimica Acta (2020) 187: 25
https://doi.org/10.1007/s00604-019-3882-y

ORIGINAL PAPER

# Electrochemiluminescence methods using CdS quantum dots in aptamer-based thrombin biosensors: a comparative study

Ibrahim Isildak[1] · Farzaneh Navaeipour[2] · Hadi Afsharan[2] · Gulsah Soydan Kanberoglu[3] · Ismail Agir[4] · Tugba Ozer[1] · Nasim Annabi[5] · Eugenia Eftimie Totu[6] · Balal Khalilzadeh[7,8]

Received: 26 May 2019 / Accepted: 29 September 2019 / Published online: 6 December 2019
© Springer-Verlag GmbH Austria, part of Springer Nature 2019

## Abstract

The detection of thrombin by using CdS nanocrystals (CdS NCs), gold nanoparticles (AuNPs) and luminol is investigated in this work. Thrombin is detected by three methods. One is called the quenching method. It is based on the quenching effect of AuNPs on the yellow fluorescence of CdS NCs (with excitation/emission wavelengths of 355/550 nm) when placed adjacent to CdS NCs. The second method (called amplification method) is based on an amplification mechanism in which the plasmonics on the AuNPs enhance the emission of CdS NCs through distance related Förster resonance energy transfer (FRET). The third method is ratiometric and based on the emission by two luminophores, viz. CdS NCs and luminol. In this method, by increasing the concentration of thrombin, the intensity of CdS NCs decreases, while that of luminol increases. The results showed that ratiometric method was most sensitive (with an LOD of 500 fg.mL$^{-1}$), followed by the amplification method (6.5 pg.mL$^{-1}$) and the quenching method (92 pg.mL$^{-1}$). Hence, the latter is less useful.

**Keywords** CdS Nanocrystals · Gold nanoparticles · Ratiometric biosensor · Thrombin · Aptamer · Electrochemiluminescence

## Introduction

Analysis, detection, and quantification of biomolecules which have great impacts on people's health, are often being carried out by biosensors all around the world [1–3]. The use of biosensors is not just limited to health-related applications, it also plays crucial role in genetic surveillance, food quality, drug monitoring and environmental monitoring [4–7]. Electrochemical [8–11], optical [12], and electrochemiluminescent (ECL) methods are quite common [2]. The ECL technique has some advantages compared to other methods, making it as a promising approach for clinical detection. Relatively low-cost, versatility, high sensitivity, great optical amplification setup, low background signal, good selectivity and biocompatibility, better efficiency, and

**Electronic supplementary material** The online version of this article (https://doi.org/10.1007/s00604-019-3882-y) contains supplementary material, which is available to authorized users.

✉ Ibrahim Isildak
isildak@yildiz.edu.tr; iisildak@gmail.com

✉ Balal Khalilzadeh
khalilzadehb@tbzmed.ac.ir; Balalkhalilzadeh@gmail.com

[1] Department of Bioengineering, Faculty of Chemistry-Metallurgy, Yildiz Technical University, 34220 Istanbul, Turkey

[2] Faculty of Physics, Iran University of Science and Technology, Tehran 16846-13114, Iran

[3] Department of Chemistry, Faculty of Science, Yuzuncu Yil University, 65080 Van, Turkey

[4] Bioengineering Department, Istanbul Medeniyet University, Goztepe, 34700 Istanbul, Turkey

[5] Chemical and Biomolecular Engineering Department, University of California, Los Angeles, CA 90095, USA

[6] Faculty of Applied Chemistry and Material Science, University Politehnica of Bucharest, 11061 Bucharest, Romania

[7] Stem Cell Research Center, Tabriz University of Medical Sciences, Tabriz 51664-14766, Iran

[8] Biosensors and Bioelectronics Research Center, Ardabil University of Medical Sciences, Ardabil 56189-85991, Iran

reliability are some of these paramount advantages [3, 13]. Beside all of these, utilizing novel methods in ECL biosensors make it even more interesting. Conventional ECL methods have been used extensively by the researcher to detect different types of biomolecules. Some interesting biosensors which were applied for detection of thrombin, have been highly noticed by research groups in this filed [14–19]. These conventional techniques include quenching method (QM) and amplification method (AM) [20, 21]. The QM has very basic mechanism that uses luminophores to sense target biomarkers or biomolecules. In this method, more concentration of the target is equal to lesser ECL signal. On the other hand, in AM, the amplification of ECL signal of luminophores by the use of nanoparticles (for example usage of gold nanoparticles) causes ECL intensity to become more intense. As indicated by the name of this method, more target biomolecules would end in higher ECL signal. These two methods are applied extensively in immunoassay, DNA detection, cancer screening, and environmental analysis [22].

We took a further step forward and used a mechanism called ratiometric method (RM). Ratiometric method, in which the quantification depends on the ratio of two signals instead of absolute values of one luminophore, is relatively a new assay used in biosensing [17, 23, 24]. Here, we applied CdS nanocrystals (CdS NCs) and luminol as two luminophores creating ECL signals. The CdS NCs have some incredible characteristics, which enable them to be quenched or amplified by gold nanoparticles (AuNPs). When CdS and AuNPs are in an approximately close range, quenching effects happen due to the non-radiative energy dispersion and Förster resonance energy transfer (FRET). In contrast, amplification phenomenon takes place when AuNPs and CdS are at certain distance in account of AuNPs- surface plasmon resonance (SPR). ECL of the CdS induces the SPR of AuNPs, which in return, amplifies the ECL response of CdS [13]. In this CdS-AuNPs group, CdS is ECL donor and AuNPs are ECL acceptors [25, 26].

Thrombin was taken into consideration and measured by ECL biosensors by utilizing QM, AM and RM strategies. Thrombin is a serine protease, a well-known target for anticoagulation and cardiovascular disease therapy, that plays crucial role in many life processes, including blood coagulation, incrustation and inflammation, and causes some diseases such as Alzheimer's [27]. A picomolar level of thrombine in human blood could cause various illnesses [28]. The blood detection of thrombin is essential for the assessment of the effectiveness of therapeutic medicine as well as for the patients with diseases associated with coagulation abnormalities. Furthermore, and more importantly, thrombin is used to help control bleeding during surgery. Therefore, detection and measurement of thrombin is extremely crucial in research as well as in clinical diagnosis [26, 29]. Here, we compared the results recorded for thrombin defection from ECL biosensors using three different methods: QM, AM, and RM. In the QM, CdS was immobilized on the electrode and thrombin was introduced to it using a capture aptamer coupled with AuNPs. The presence of thrombin ended in adjacent AuNPs to CdS. In AM, after immobilizing CdS on the electrode surface, thrombin was sandwiched between a capture aptamer and a reporter aptamer conjugated with AuNPs. The final approach consisted of both features. In the presence of thrombin, CdS was quenched because AuNPs on the capture aptamer was so close to them, and luminol was introduced through the completion of sandwich formation. Subsequently, two ECL signals were detected on the output. This method worked perfectly since both CdS and luminol were working with $H_2O_2$ as their substrate and have completely separated triggering potential [13]. The main target of the present study was to assess which approach is better with improved performance.

## Experimental

### Materials and reagents

Labeled DNA oligonucleotides were synthesized according the sequences represented below and received from Sangon Biotechnology Co. Ltd. (Shanghai, China):

Aptamer I: 5 − HS − $(CH_2)_6$ − GGT TGG TGT GGT TGG − 3 - biotin
Aptamer II: 5 − biotin − AGT CCG TGG TAG GGC AGG TTG GGG TGA CT − 3

Tri (2-carboxyethyl) phosphine hydrochloride (TCEP), gold chloride tri-hydrate ($HAuCl_4.3H_2O$), bovine serum albumin (BSA, purity ≥98%), cadmium nitrate tetra hydrate ($Cd(NO_3)_2{\cdot}4H_2O$), hydrogen peroxide ($H_2O_2$), luminol and thrombin were purchased from Sigma-Aldrich (St. Louis, MO, USA, www.sigmaaldrich.com/united-states.html). Citric acid and trisodium citrate were bought from Merck (Hohenbrunn, Germany, www.merckmillipore.com). Streptavidin was obtained from Abcam (Cambridge, USA, www.abcam.com). $Na_2S.xH_2O$ (32–38%) was received from Fluka (Switzerland, www.lab-honeywell.com/products/brands/fluka). Phosphate buffer solution (PBS) was prepared by dissolving 0.137 M NaCl, 0.1 M $Na_2HPO_4$, 0.0018 M $KH_2PO_4$ and 0.0027 M KCl in one liter distilled water (DW). NaOH was used to adjust the pH of PBS before storing it at 4 °C. All chemicals necessary for pH adjustment were purchased from Merck (Hohenbrunn, Germany, www.merckmillipore.com).

### Apparatus and equipment

Differential pulse voltammetry (DPV) experiments were carried out using an Auto-Lab (PGSTAT12 (Eco-chemie, BV, The Netherlands)) with three conventional electrodes, a glassy carbon electrode (GCE) as working electrode, an Ag/AgCl as reference electrode, and a platinum rode as the counter electrode. The ECL measurements were performed in a dark room and at 25 °C using an Elecsys 2010 (Roche/Hitachi, Mannheim, Germany). The voltage of the photomultiplier (PMT) was adjusted to 800 V during the test. Scanning electron microscopy (SEM) images were taken using a Zeiss EVO® LS 10 (Germany). UV-visible and photoluminescence spectra were recorded by Pharma Biotech (United Kingdom) and JASCO (Japan), respectively.

All of the synthesis process of CdS NCs, AuNPs and modification of AuNPs with streptavidin and luminol were explained in detail in the Electronic Supporting Material (ESM) section.

### Biosensor preparation applying different methods and their ECL biosensing procedures

The fabrication of the ECL biosensor was performed according to Scheme 1 using three different procedures including: QM, AM, and RM.

In all three methods, the first step was to polish and wash GCE carefully with alumina powder and DW three times to obtain a clear and clean surface. Next, 20 μL CdS drop-casted on the GCE and dried at room temperature. As described before [30], we activated GCE/CdS prior any further modification. CdS is activated by an activating buffer containing $H_2O_2$ and citric acid. This results in 58 times greater ECL emission in comparison to that of conventional (without activation) approach. After this step, the first aptamer (the capture probe I) was immobilized on the engineered electrode by soaking the GCE/CdS in a 20 μL solution of the aptamer I (5 μM) for almost 12 h at 4 °C with 100% humidity [13, 31]. For the activation of –SH group on the aptamer I, 25 μL TCEP was utilized. These modification steps were applied for all the methods utilized for the biosensor fabrication explained below.

In the QM, streptavidin modified AuNPs (Str-AuNPs) was added to the GCE/CdS/aptamer I by incubating at 4 °C for 4 h. Afterward, the electrode was submerged in BSA (1% *w/v*) to block any unspecific binding sites. Finally, and after adding thrombin to the GCE/CdS/aptamer I/AuNPs, the ECL of CdS was quenched due to the distance related effect of CdS and AuNPs and the fact that the ECL of CdS was transferred into AuNPs' metal core by non-radiative energy dispersion. In other word, more thrombin is equal to more quenching and less ECL intensity.

In the AM, after blocking with BSA, thrombin was drop-casted on GCE/CdS/aptamer I. Next, 20 μL of the designed aptamer II-str-AuNPs was introduced to the modified electrode upon soaking for 20 min at room temperature with 100% humidity. In this method, more thrombin produced higher ECL intensity since the ECL of CdS gives rise to more SPR of AuNPs, resulting in an increase amplifying the ECL response of CdS.

In the RM, similar to QM, GCE/CdS/aptamer I was incubated with str-AuNPs at 4 °C for 4 h. Afterward, the electrode was soaked in a BSA (1% *w/v*) solution to minimize the unspecific binding. Then, thrombin added to the engineered electrode. After adding 20 μL aptamer II-str-Lum-AuNPs by immersing the electrode for 20 min under 100% humidity, the ECL measurements were performed. Similar to QM, adding more thrombin resulted in the ECL quenching of CdS, but here, and unlike the first method, this increment in the thrombin concentration resulted in an increase in the ECL of luminol.

It is worth mentioning that, all the probes and thrombin were kept at room temperature for 10 min prior to use. Furthermore, after each step of modification, the electrodes were washed by immersing in PBS (pH = 7.5) for 10 min in order to flush the unreacted materials.

The ECL experiments were performed in PBS containing $H_2O_2$ (the co-reactant of both luminol and CdS) from −0.8 to −1.5 V in QM and AM, and from −1.5 to 0.8 V in the RM at 0.1 V. $s^{-1}$. During these measurements, the applied potential to photomultiplier (PMT) was adjusted to 800 V.

## Results and discussion

### Characterization of the materials

It is important to first evaluate the authenticity of synthesized materials before using them for engineering a biosensor. Therefore, we assessed the synthesized CdS, AuNPs, str-Lum-AuNPs and str-AuNPs by different methods including SEM, UV-visible and photoluminescence (PL) spectra.

CdS NCs were firstly investigated by taking SEM images. As it is shown Fig. S1A (see in Supplementary material), the nanoparticles diameter is about 20 nm. These particles are spherical. Further assessments were performed by UV-visible and PL (see in Supplementary material and Fig. S1B and S1C). A slight peak at 480 nm observed in the UV-visible spectrum of CdS nanocrystals can be attributed to CdS according to the prior studies [32, 33]. The PL spectra (355 nm was used for excitation) also showed some characteristic peaks at near 500 nm and a strong emission at 550 nm. These peaks are unique to CdS nanoparticles synthesized in our paper. Also,

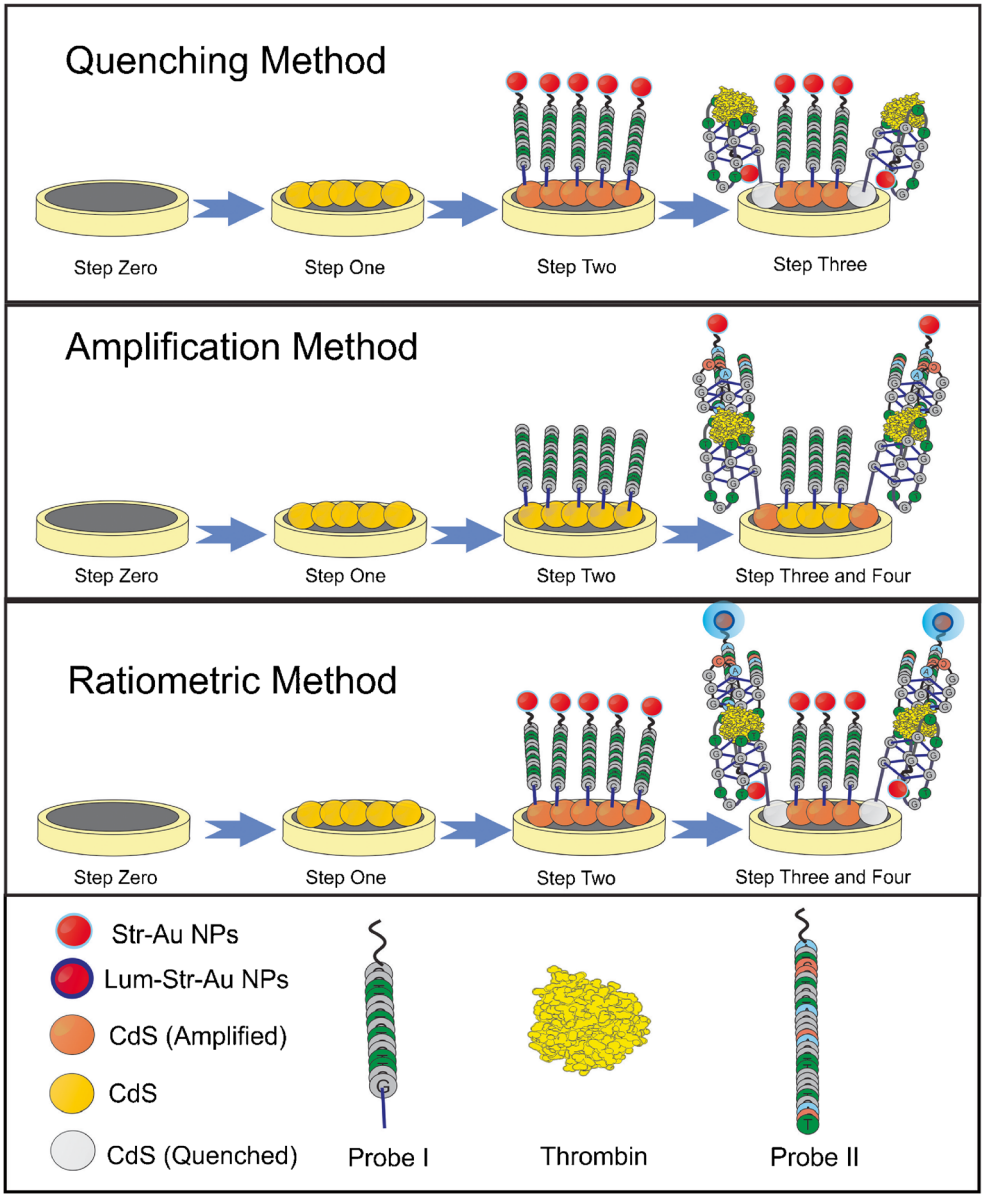


**Scheme 1** Schematic illustration of prepared ECL biosensor in QM, AM and RM

these data are consistent with other literatures [25, 32]. AuNPs, str-AuNPs and str-Lum-AuNPs authenticity were evaluated by different methods. SEM images showed the morphology of these synthesized particles. According to Fig. S2A (see in Supplementary material), AuNPs had spherical shapes and were around 50 nm. After treating these synthesized AuNPs with luminol, the size of the nanoparticles became slightly larger (see in Supplementary material and Fig. S2B). For the streptavidin modified AuNPs (str-AuNPs), is shown in Fig. 2c, after modification of streptavidin, the size of the particles has experienced an increment.

Furthermore, UV-visible spectra of AuNPs was compared to that of luminol (see in Supplementary material and Fig. S3A). Acquired spectra showed that while AuNPs had only a peak at 525 nm (which is due to the SPR on the AuNPs surface), the luminol-AuNPs created two other absorption peaks at 300 and 350 nm, while the peak of AuNPs is still observed at 550 nm. In addition, since AuNPs had no PL activity, only luminol-AuNPs had an emission on PL spectra (see in Supplementary material and Fig. S3B).

These data together confirm that AuNPs, str-AuNPs and str-Lum-AuNPs were synthesized correctly through the experiments.

## Electrochemical characterization of the modified electrodes

Electrochemical behavior (DPV) of the modified electrodes (is shown in Fig. 1) using different methods were taken in a solution of PBS (0.1 M, pH = 7.5) containing the standard

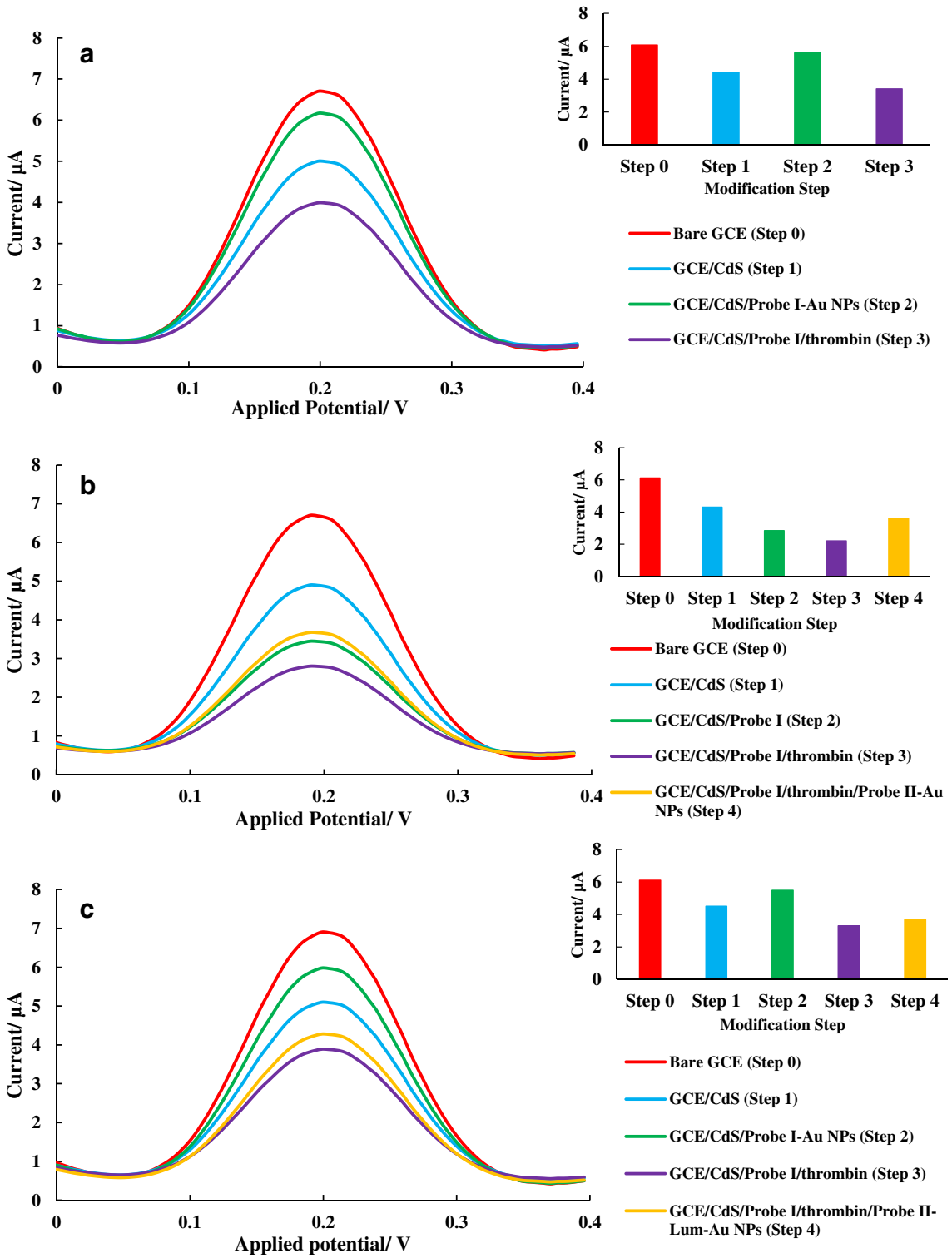


**Fig. 1** The DPV curves of the biosensor in **a** QM, **b** AM, and **c** RM at different preparation steps in PBS (0.1 M, pH = 7.5) containing 5 mM $K_4[Fe(CN)_6]$, $K_3[Fe(CN)_6]$ and 0.1 M KCl at scan rate of 100 $mV.s^{-1}$ (Insets: The peak current versus preparation steps)

solution of 5 mM $K_4[Fe(CN)_6]$, $K_3[Fe(CN)_6]$ and 0.1 M KCl at 100 $mV.s^{-1}$. As shown in Fig. 1a, in the QM, the peak of the bare GCE decreased after adding CdS on the electrode as expected. This is because CdS has insulating characteristics that hinder the electron transfer. Adding probe I-AuNPs resulted in an increment in the recorded DPV peak, showing the effect of AuNPs on facilitating the electron transference rate. Finally, and after the introduction of thrombin, the DPV curve and peak were further declined that was attributed to the attachment of thrombin by the aptamer.

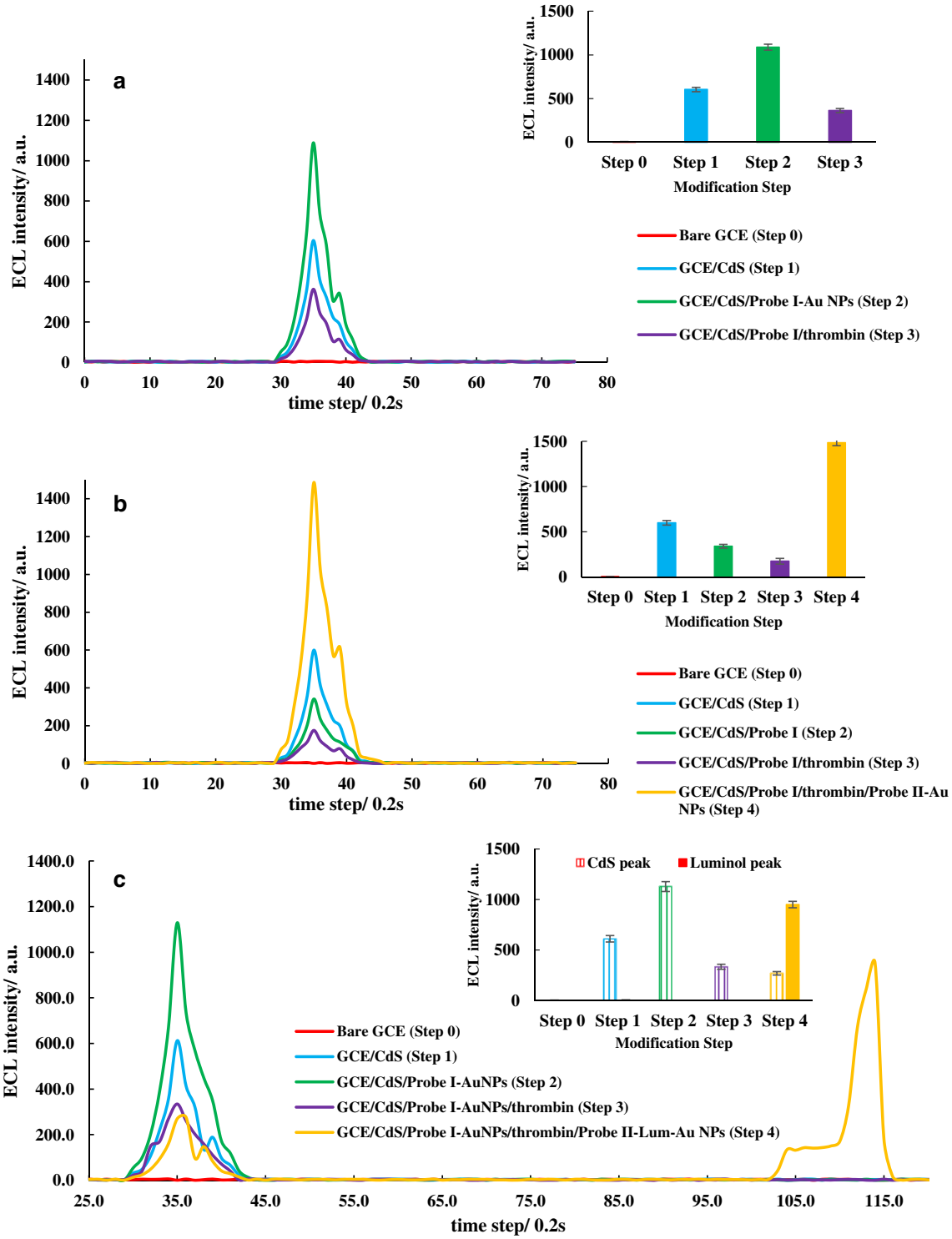


**Fig. 2** The ECL responses of the thrombin biosensor at various modification steps in **a** QM, **b** AM, and **c** RM in a PBS (0.1 M, pH = 7.5) containing 25 mM $H_2O_2$ (Insets: The ECL peak intensities versus modification steps)

For the AM (Fig. 1b), the same behavior is predicted. After adding CdS, probe I and thrombin, the recorded DPV peaks experienced a decline, while after adding probe II-AuNPs, a small increment was observed in the curves.

Finally, for the RM, the changes were the combination of two previous methods. Briefly, adding CdS, probe I-AuNPs, thrombin, and probe II-Lum-AuNPs resulted in a decrease, increment, decrease and an amplification to the DPV peaks (Fig. 1c). Here and at the

final step, AuNPs played a crucial role as conductors to heighten the electron transfer.

## Electrochemiluminescence characterization of the organized thrombin biosensor

The ECL characterization of the suggested methods are shown in Fig. 2. In all the three methods, after drop-casting CdS (step 1), the ECL intensity raised in the presence of $H_2O_2$. Separately, in QM (Fig. 2a), in the second step (adding probe I-AuNPs), the ECL emission increased, showing the amplification impact of AuNPs on the ECL of CdS. Obviously and after adding thrombin as the main analyte (step 3), the recorded photons decreased due to the quenching effects of AuNPs on CdS in a close range. In other words, where thrombin is present, aptamer-thrombin interaction ended in a folding, bringing the AuNPs close enough to CdS NCs and quenching the ECL of CdS [27].

According to AM (Fig. 2b), step 2 and 3 (adding Probe I and thrombin, respectively) ended in further decline in the observed ECL intensity. Both due to the electron hindrance impacts of probe I and thrombin. Finally, by introducing probe II-AuNPs to the modified electrode, the AuNPs-enhanced Raman scattering made ECL of CdS to be amplified extensively.

In RM, we took advantage of both QM and AM concurrently. Therefore, after the second step, adding probe I-AuNPs, the ECL peak experienced an increment due to the SPR effects of AuNPs. Step 3 made the ECL peak to drop due to the presence of thrombin. Thrombin not only did cover the electrode surface and decreased electron transfer rate, but also resulted in quenching of CdS ECL like what happened in QM. Finally, drop casting probe II-lum-AuNPs decreased the ECL peak of CdS. On the other hand, an ECL intensity of luminol was observed in the ECL output. The decrease in CdS ECL intensity because of Probe II, while approaching a peak in the ECL curves can be interpreted as the fully introduction of luminol to the electrode surface. These curves are shown in Fig. 2c. The results of electrochemical characterization confirmed the authenticity of electrode preparation.

## Electrochemiluminescence behavior of the planned immunosensor in ratiometric method

The following details are explained here to better clarify how the immunosensor in RM works.

Consider the equations pertinent to CdS and $H_2O_2$ group:

$$CdS + ne^- \rightarrow n(CdS)^{\cdot -}$$

$$H_2O_2 + e^- \rightarrow OH^- + OH^{\cdot}$$

$$(CdS)^{\cdot -} + OH^{\cdot} \rightarrow (CdS)^{*} + OH^-$$

$$(CdS)^{*} \rightarrow (CdS) + h\nu$$

By applying a negative potential (around −1.2 V), $(CdS)^{\bullet -}$, and $OH^{\bullet}$ were produced at the electrode surface. After that, OH• reacted with $(CdS)^{\bullet -}$ which resulted in the formation of the (CdS)* excited state. This excited CdS emits photons and returns to its ground state. One of the advantages of this procedure is the continuous and free formation of $H_2O_2$ by electrochemical reduction of oxygen in aqueous solution [30]. Furthermore, the ECL of CdS nanocrystals can easily be quenched or amplified when AuNPs are in a close distance or are in a relatively long distance (in the biomolecules scale). As mentioned before, the induction of SPR in AuNPs causes the ECL photons to become bolstered [34].

On the other hand for the luminol and $H_2O_2$ groups we have [35]:

$$H_2O_2 - e^- \rightarrow \frac{1}{2} O_2^{\bullet -} + H_2O$$

$$LumH_2 + OH^- \rightarrow LumH^- + H_2O$$

$$LumH^- - e^- \rightarrow LumH^{\bullet} \rightarrow Lum^{\bullet -} + H^+$$

$$Lum^{\bullet -} + O_2 \rightarrow O_2^{\bullet -} + Lum$$

$$Lum^{\bullet -} + O_2^{\bullet -} \rightarrow LumO_2^{2-}$$

$$LumO_2^{2-} \rightarrow AP^{2-*} + N_2$$

$$Ap^{2-*} \rightarrow Ap^{2-} + h\vartheta(425\ nm)$$

The presence of $OH^{\bullet}$, $O_2^{\bullet -}$ and singlet oxygen ($^1O_2$) are vital for ECL emission of luminol and therefore enrichment of them can result in more and more photon emission [36]. According to the equations (in the aqueous solution), at the electrode surface luminol anion ($LumH^-$) reduces to the luminol radical anion ($Lum^{\bullet -}$), followed by further oxidation of $Lum^{\bullet -}$ to the excited state 3-aminophthalate species ($AP^{2-*}$), which can subsequently emit light. Simultaneously at the electrode surface, oxidation of $H_2O_2$ electrode surface can result in the formation of $O_2^{\bullet -}$. The formed $O_2^{\bullet -}$ reacts with $L^{\bullet -}$ and generates $AP^{2-*}$ molecules, resulting in amplification of ECL emission [37].

## Finding the optimum pH value

The ECL intensity and as a result, the sensitivity of the immunosensor is highly dependent on pH of the solution. Effect of pH on the ECL response of the offered methods was therefore investigated.

In the QM, ECL curves carried out with an electrode with 1000 pg.mL$^{-1}$ thrombin in a PBS solution containing 25 mM $H_2O_2$ with different pH values from 5.0 to 10.0. The data are shown in Fig. S4A (see in Supplementary material). Accordingly, pH = 7.5 was obtained as the optimal value and used in QM measurements. In the case of AM, the same PBS with different pH was used and similarly, 7.5 were derived as the optimum value (see in Supplementary material and Fig. S4B). As shown in Fig. S4 (see in Supplementary material), as the acidic environment disrupted the CdS functionality and at

the same time was harmful for biomolecules like thrombin, ECL intensity showed an increment in the pH values of 5.0 to 7.5 and then decreased. Also, higher pH values caused an instability to $H_2O_2$. In addition, the biomolecules including thrombin and probe I and II worked better under physiological conditions, so higher pHs can result in lower ECL emission.

Finally, for the RM, the electrode containing 100 pg.mL$^{-1}$ thrombin was placed in PBS (0.1 M, 25 mM $H_2O_2$) with various pH. The recorded ECL curves and intensities are displayed (see in Supplementary material and Fig. S4C). Since there are two peaks in the ECL of RM, the gained pH value is highly dependent on the optimal pH values of both CdS and luminol peaks. The optimum value for CdS was 8.0, while that of luminol was obtained at pH = 9.0. Acceleration in formation of luminol radicals from luminol was the reason behind why higher pH values are equal to more CdS ECL. Because of this, the ECL peak was achieved higher in higher pH. On the other hand, alkaline environments were not good for thrombin and aptamers, so an increase in pH of the PBS was harmful and could lead to lower emitted photons. Consequently, 8.5 was considered as the optimized pH. These data and conclusions here are consistent with other literatures [3, 25, 37].

## $H_2O_2$ concentration optimization

Since the ECL responses of the CdS and luminol are dependent on the $H_2O_2$ concentration in PBS, we carried out the experiments to evaluate and obtain the optimal $H_2O_2$ concentration. To do this, in QM and AM, the electrode was prepared using 1000 pg.mL$^{-1}$ thrombin and used as the working electrode in a PBS (0.1 M, pH = 7.5) with different concentrations of $H_2O_2$ (5, 10, 15, 20, 25, 30, 35, 40 and 50 mM) at 0.1 V. s$^{-1}$. The resulted ECL intensities and peaks are presented in Supplementary material, Fig. S5A and Fig. S5B, respectively. Increasing the concentrations of $H_2O_2$ to 20 mM led to an increment in ECL peaks, while further increment did not affect the peaks so much. In other words, the peaks stood still. The reason of such behavior can be related to the saturation of $H_2O_2$ reactions on the electrode surface which resulted in a constant number of CdS excited state molecules and consequently, a steady ECL intensity to be recorded. Based on these data, the optimum concentration of $H_2O_2$ for both QM and AM was 20 mM.

The same test was carried out for RM with an electrode set using 100 pg.mL$^{-1}$ of thrombin (see in Supplementary material and Fig. S5C). Similar to the QM and AM methods, the peak of CdS increased first and then reached a plateau. Based on these peaks, 25 mM was obtained as optimum value. But the optimum value for the luminol peak was 30 mM. Since there were not observed significant differences between the peaks recorded for 25 mM and 30 mM CdS, then the 30 mM concentration was as optimum concentration for $H_2O_2$ experiments and used in all RM tests.

## Immunosensor performances

Performance was evaluated under optimized conditions as follow.

a. Quenching Method:

The electrode was prepared using different concentrations of thrombin in PBS (0.1 M, pH = 7.5) in the presence of 20 mM $H_2O_2$. The ECL responses and peak intensities gathered from CdS NCs in QM are shown in Fig. 3a. It can be seen that higher thrombin concentrations (from 500 to 5000 pg.mL$^{-1}$) led to lower ECL peaks. It was obvious that more thrombin supplied on the electrode can result in more CdS molecules being quenched by AuNPs adjacent to them. The associate LOD of the QM calculated was as 92 pg.mL$^{-1}$.

b. Amplification Method:

In this method, the electrode was engineered with different concentrations of thrombin including 50, 100, 150, 200, 250, 500 and 1000 pg.mL$^{-1}$. Unlike the QM, here the ECL peaks experienced a raise while the concentration of thrombin increased (Fig. 3b). This behavior is due to the fact that higher concentration of thrombin on the electrode causes more CdS NCs to be amplified through SPR of the AuNPs (because they are in specific distance with each other) by providing possible SPR. This, in turn, enhances the performance. The LOD for this method was about 6.5 pg.mL$^{-1}$ which indicated a better performance compared to QM.

c. Ratiometric Method:

In this method, the electrode was designed with different concentrations of thrombin (5, 10, 20, 25, 50, 100, 200 and 500 pg. mL$^{-1}$) and their ECL intensities were measured. As shown in Fig. 4a and b, higher concentration of thrombin resulted in higher luminol's ECL peak and at the same time, lower CdS's ECL intensity. The luminol of ECL was increased because more thrombin enhancing luminol concentration to the electrode surface and more photons are being emitted from luminol. The ECL of luminol was also enhanced because of the presence of AuNPs at the end of probe II near luminol. These AuNPs played conductors role and facilitated the electron transfer rate. On the other hand, due to the quenching effect of AuNPs on CdS ECL through Förster resonance energy transfer (FRET), the ECL of CdS NCs was reduced since more thrombin, means more folded probe I, and consequently more AuNPs close to CdS. This method can be used in account of the fact that, both ECL of luminol and CdS can be distinguished clearly and there was almost no interference between these two. The ECL of CdS was observed at −1.25 V, while that of luminol was observed near

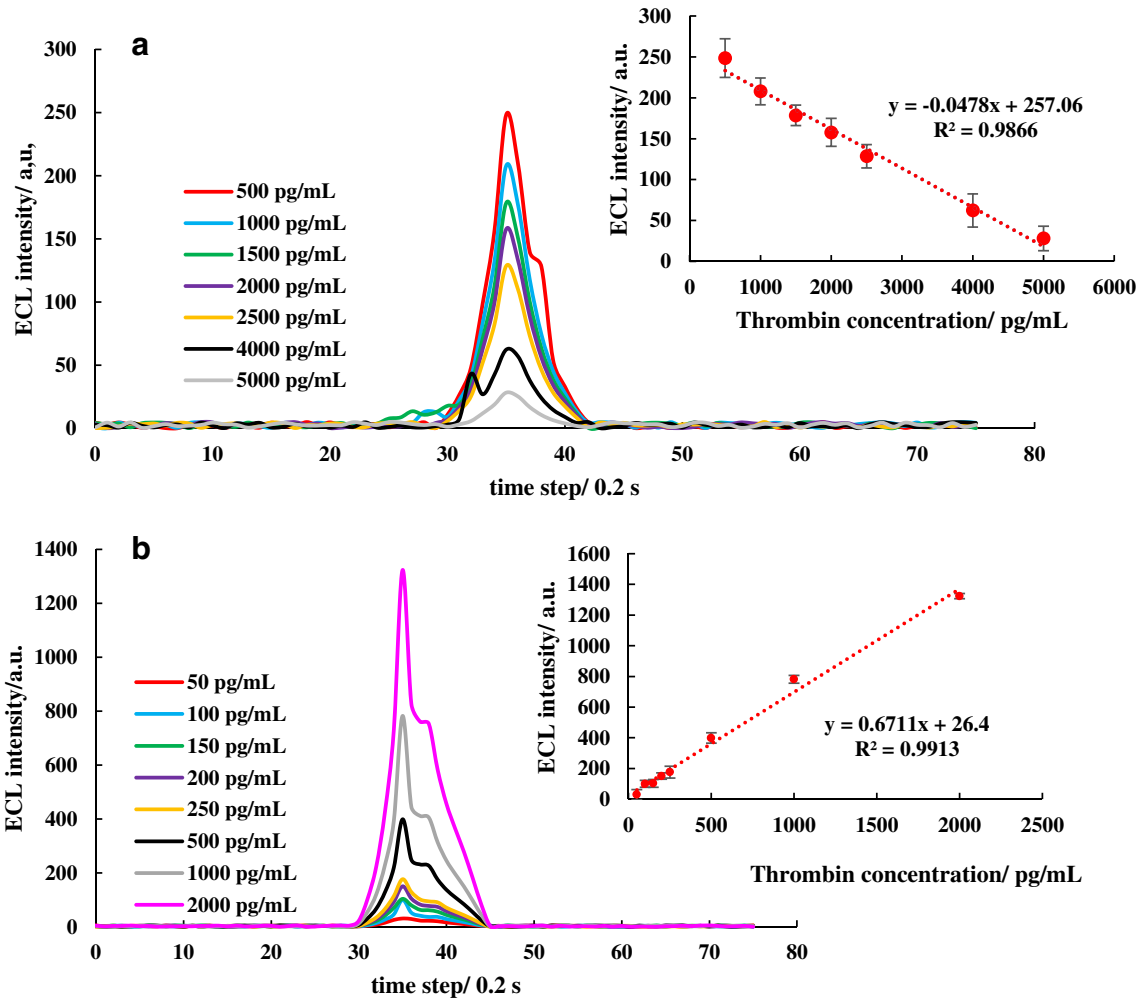


**Fig. 3** The performance of the thrombin biosensor in detection of different concentrations of thrombin in **a** Quenching Method and **b** Amplification Method. Insets are the calibration curve for the QM and AM, respectively. Experiments were carried out in PBS (0.1 M, pH = 7.5) containing 20 mM $H_2O_2$ at 0.1 $V.s^{-1}$ in QM and AM

0.4 V. The LOD of this RM was calculated based on the ECL intensity of luminol/ ECL intensity of CdS. This LOD was about 500 $fg.mL^{-1}$. Table 1 compares the results got in the current work with those for thrombin detection from literature.

When it comes to comparison, it is obvious that the performance of the RM was better than quenching and amplification methods. The recorded LODs sustain the RM method performance. This behavior is explained by the fact that in our RM, when two luminophores (luminol and CdS) were used, the emitted photons were more effective than in the case when CdS was used alone. In other words, in the QM, the presence of thrombin was detected indirectly (through the quenching of CdS), while in the AM, the presence of thrombin was directly monitored (more thrombin equals to more CdS ECL intensity). However, in the RM, not only the presence of thrombin was measured through luminol ECL directly, but it was also being detected indirectly through ECL of CdS, at the same time. As a result of this, more accurate data were gathered from RM which resulted in better and highly sensitive detection. In other words, the presence of thrombin was double checked using RM. In the QM and RM, the detection was usually based on a single emission intensity changes which can be affected by false positive or negative errors due to instrumental efficiency or some environmental changes. Furthermore, the use of AuNPs-luminol amplified the ECL of luminol.

## Interference study for the ratiometric method

For the selectivity test, the interference impact of different agents was investigated for the fabricated biosensor in RM. These interfering agents were IgG, bovine serum albumin (BSA) and human serum albumin (HSA). To compare the modified electrode selectivity, the results achieved by the presence of these agents were compared to that of 100 $pg.mL^{-1}$ thrombin. Figure 5 shows that there was almost no luminol peak intensity when interfering agents were used, while very intense peaks of CdS were observed. Similarly,

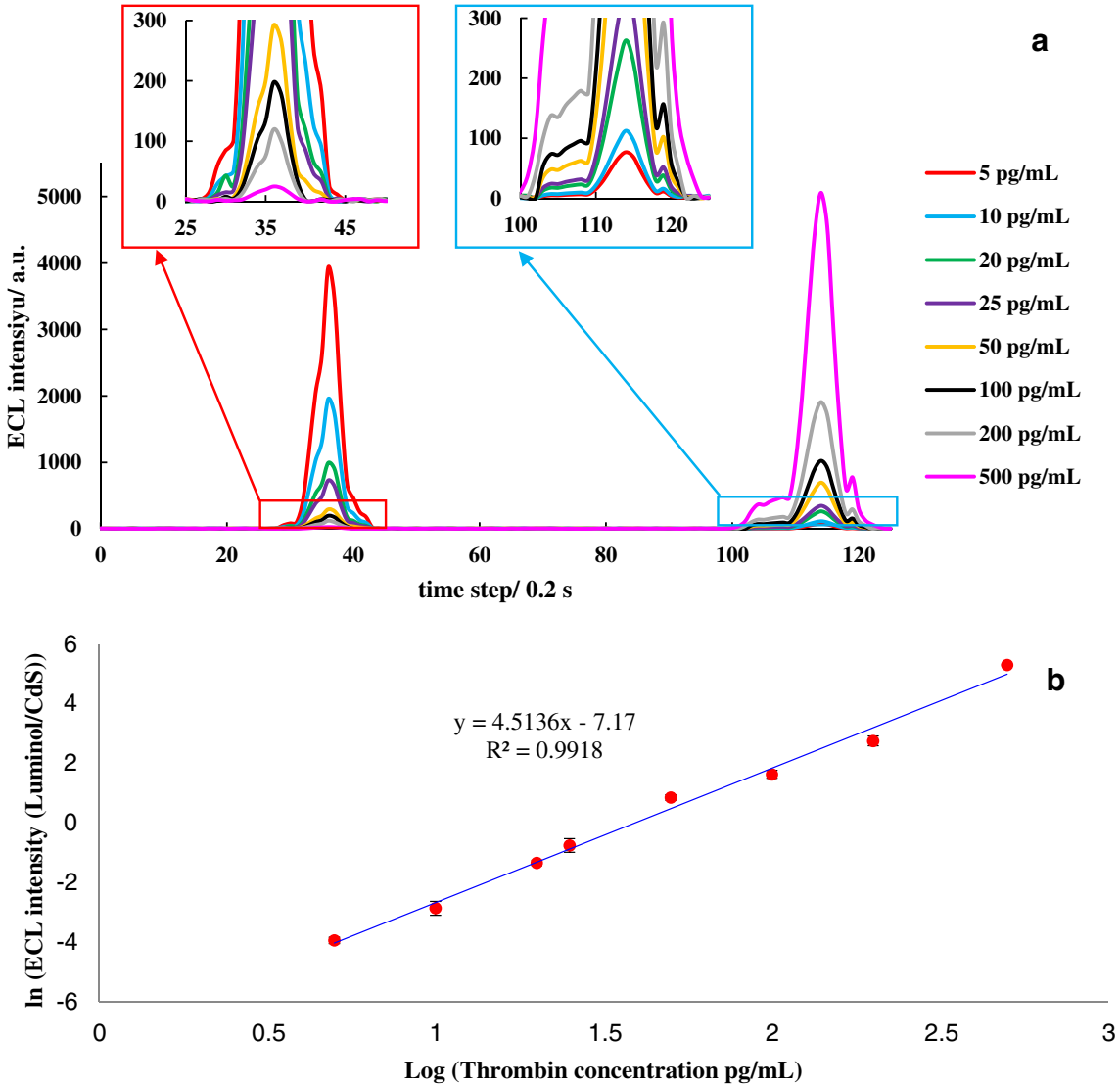


**Fig. 4** **a** The performance of the thrombin biosensor in detection of different concentrations of thrombin in RM. **b** the calibration curve obtained for the RM in detection of thrombin. The experiments were carried out in PBS (0.1 M, pH = 8.5) containing 30 mM $H_2O_2$ and at scan rate of 0.1 $V.s^{-1}$

**Table 1** Performance of the thrombin biosensor designed in this article compared with those introduced in other reported literatures

| Type of the ECL biosensor | Detection Limit | Reference |
|---|---|---|
| Quenching ECL | 10 nM | [38] |
| Quenching ECL | 1.7 pM | [39] |
| Ratiometric ECL | 4.2 fg/mL | [40] |
| Amplification ECL | 0.21 nM | [28] |
| Amplification ECL | 6.3 pM | [41] |
| Quenching ECL | 1.7 pM | [29] |
| Amplification ECL | 2 pM | [27] |
| Quenching ECL | 92 $pg.mL^{-1}$ (≤2.6 pM) | This Work |
| Amplification ECL | 6.5 $pg.mL^{-1}$ (≤0.18 pM) | This Work |
| Ratiometric ECL | 500 $fg.mL^{-1}$ (≤0.014 pM) | This Work |

when no thrombin was immobilized on the electrode, the peak for luminol was almost subtle. These data indicated that the engineered biosensor showed almost no response to the other proteins.

## Determination of thrombin using the ratiometric method in real samples

The performance of the electrode was further evaluated in real samples containing different concentrations of thrombin. In this sense, different electrodes were prepared by various thrombin samples. The samples were prepared by standard addition method. The data gained from these electrodes are summarized in Table 2. It can be seen that the biosensor had high performance when used in real samples. The calculated RSD ranged between −3.97 and 7.68% that is satisfactory.

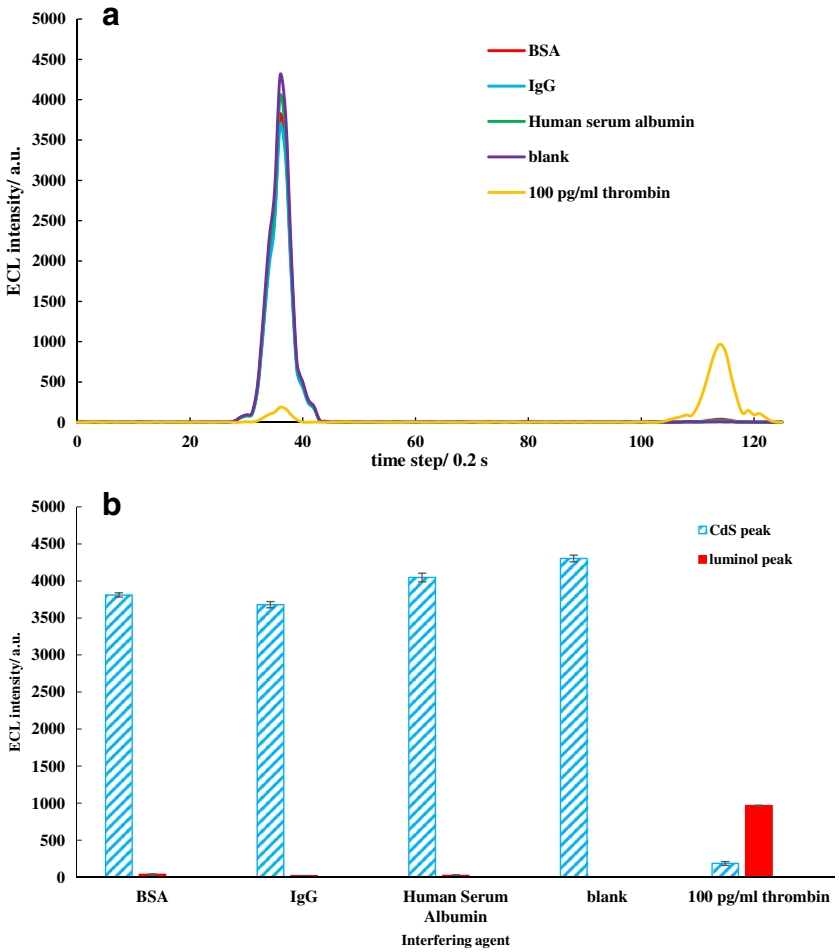


**Fig. 5** Selectivity investigation of the biosensor by comparing the ECL responses of the engineered electrode incubated in different interfering agents including BSA, HSA, IgG and 100 pg.ml$^{-1}$ thrombin and the blank electrode in PBS (0.1 M, $p = 8.5$) containing 30 mM $H_2O_2$

## Conclusion

Thrombin was detected by using three different ECL methods. The technique containing CdS-AuNPs group has a unique characteristic: when it is in a close approximate, the ECL of CdS was quenched by AuNPs, and when in a specific distance, the ECL intensity would be amplified by SPR of AuNPs. In the first method, quenching method (QM), we used the quenching mechanism and measured thrombin in low concentration. In the second one, amplification method (AM), the second characteristic of CdS-AuNPs group was exploited. In this approach, by utilizing a sandwich type aptamer-based biosensor, we put AuNPs in a distance with CdS which ended in an ECL intensity amplification. The third method presented which is called a ratiometric method (RM), the biosensors benefited from both ECL of CdS (quenching) and ECL of luminol. The mechanism could be summarized as follows: thrombin was present at the electrode, through folding the capture aptamer, CdS photons were quenched and luminol emitted photons started to get produced. This procedure was found to be a useful approach in future diagnosis since it showed great selectivity and good authenticity in real samples. We anticipate that employing enhanced ECL for luminol (using luminol and HRP together) and the use of other materials (such as graphene derivatives, nonporous or/and nanoparticles) in fabrication leads to even more powerful analytical tools. The assessment of the drawbacks for the presented work highlighted the limitation due to the inaccessibility to ECL equipment and lack of specificity study of

**Table 2** Detection of thrombin by the biosensor in spiked real samples

| Added concentration (pg.mL$^{-1}$) | log (luminol/CdS) | Found concentration (pg.mL$^{-1}$) | % Recovery |
|---|---|---|---|
| 130 | 0.842 | 136.6 | 105.12 |
| 75 | 0.597 | 78.3 | 104.44 |
| 15 | −0.882 | 16.1 | 107.68 |
| 4.5 | −1.688 | 4.4 | 97.86 |
| 390 | 1.841 | 374.5 | 96.03 |

thrombin in the presence of its initiator, prothrombin and other related blood coagulation factors.

**Acknowledgements** The authors declare no conflict of interests.

## References


1. Khalilzadeh B, Shadjou N, Charoudeh HN, Rashidi M-R (2017) Recent advances in electrochemical and electrochemiluminescence based determination of the activity of caspase-3. Microchim Acta 184(10):3651–3662
2. Liu Z, Qi W, Xu G (2015) Recent advances in electrochemiluminescence. Chem Soc Rev 44(10):3117–3142
3. Navaeipour F, Afsharan H, Tajalli H, Mollabashi M, Ranjbari F, Montaseri A, Rashidi M-R (2016) Effects of continuous wave and fractionated diode laser on human fibroblast cancer and dermal normal cells by zinc phthalocyanine in photodynamic therapy: a comparative study. J Photochem Photobiol B Biol 161:456–462
4. Afsharan H, Hasanzadeh M, Shadjou N, Jouyban A (2016) Interaction of some cardiovascular drugs with bovine serum albumin at physiological conditions using glassy carbon electrode: a new approach. Mater Sci Eng C 65:97–108
5. Khalilzadeh B, Shadjou N, Kanberoglu GS, Afsharan H, de la Guardia M, Charoudeh HN, Ostadrahimi A, Rashidi M-R (2018) Advances in nanomaterial based optical biosensing and bioimaging of apoptosis via caspase-3 activity: a review. Microchim Acta 185(9):434
6. Nakhjavani SA, Khalilzadeh B, Pakchin PS, Saber R, Ghahremani MH, Omidi Y (2018) A highly sensitive and reliable detection of CA15-3 in patient plasma with electrochemical biosensor labeled with magnetic beads. Biosens Bioelectron 122:8–15
7. Aliakbarinodehi N, Stradolini F, Nakhjavani SA, Tzouvadaki I, Taurino I, Micheli GD, Carrara S (2018) Performance of carbon Nano-scale allotropes in detecting midazolam and Paracetamol in undiluted human serum. IEEE Sensors J 18(12):5073–5081. https://doi.org/10.1109/JSEN.2018.2828416
8. Afsharan H, Khalilzadeh B, Tajalli H, Mollabashi M, Navaeipour F, Rashidi M-R (2016) A sandwich type immunosensor for ultrasensitive electrochemical quantification of p53 protein based on gold nanoparticles/graphene oxide. Electrochim Acta 188:153–164
9. Afsharan H, Navaeipour F, Khalilzadeh B, Tajalli H, Mollabashi M, Ahar MJ, Rashidi M-R (2016) Highly sensitive electrochemiluminescence detection of p53 protein using functionalized Ru–silica nanoporous@ gold nanocomposite. Biosens Bioelectron 80:146–153
10. Babaei A, Zendehdel M, Khalilzadeh B, Abnosi M (2010) A new sensor for simultaneous determination of tyrosine and dopamine using iron (III) doped zeolite modified carbon paste electrode. Chin J Chem 28(10):1967–1972
11. Totu EE, Isildak I, Nechifor AC, Cristache CM, Enachescu M (2018) New sensor based on membranes with magnetic nano-inclusions for early diagnosis in periodontal disease. Biosens Bioelectron 102:336–344
12. Bian S, Lu J, Delport F, Vermeire S, Spasic D, Lammertyn J, Gils A (2018) Development and validation of an optical biosensor for rapid monitoring of adalimumab in serum of patients with Crohn's disease. Drug Test Anal 10(3):592–596
13. Hao N, Li X-L, Zhang H-R, Xu J-J, Chen H-Y (2014) A highly sensitive ratiometric electrochemiluminescent biosensor for microRNA detection based on cyclic enzyme amplification and resonance energy transfer. Chem Commun 50(94):14828–14830
14. Liu Y, Zhao Y, Fan Q, Khan MS, Li X, Zhang Y, Ma H, Wei Q (2018) Aptamer based electrochemiluminescent thrombin assay using carbon dots anchored onto silver-decorated polydopamine nanospheres. Microchim Acta 185(2):85
15. Wang L, Yang W, Li T, Li D, Cui Z, Wang Y, Ji S, Song Q, Shu C, Ding L (2017) Colorimetric determination of thrombin by exploiting a triple enzyme-mimetic activity and dual-aptamer strategy. Microchim Acta 184(9):3145–3151
16. Wang X, Sun D, Tong Y, Zhong Y, Chen Z (2017) A voltammetric aptamer-based thrombin biosensor exploiting signal amplification via synergetic catalysis by DNAzyme and enzyme decorated AuPd nanoparticles on a poly (o-phenylenediamine) support. Microchim Acta 184(6):1791–1799
17. Wang Y-H, Xia H, Huang K-J, Wu X, Ma Y-Y, Deng R, Lu Y-F, Han Z-W (2018) Ultrasensitive determination of thrombin by using an electrode modified with WSe 2 and gold nanoparticles, aptamer-thrombin-aptamer sandwiching, redox cycling, and signal enhancement by alkaline phosphatase. Microchim Acta 185(11):502
18. Wen C-Y, Bi J-H, Wu L-L, Zeng J-B (2018) Aptamer-functionalized magnetic and fluorescent nanospheres for one-step sensitive detection of thrombin. Microchim Acta 185(1):77
19. Xu Q, Wang G, Zhang M, Xu G, Lin J, Luo X (2018) Aptamer based label free thrombin assay based on the use of silver nanoparticles incorporated into self-polymerized dopamine. Microchim Acta 185(5):253
20. Wang X, Dong P, Yun W, Xu Y, He P, Fang Y (2009) A solid-state electrochemiluminescence biosensing switch for detection of thrombin based on ferrocene-labeled molecular beacon aptamer. Biosens Bioelectron 24(11):3288–3292
21. Yang L, Zhu J, Xu Y, Yun W, Zhang R, He P, Fang Y (2011) Electrochemiluminescence aptamer biosensor for detection of thrombin based on CdS QDs/ACNTs electrode. Electroanalysis 23(4):1007–1012
22. Khalilzadeh B, Shadjou N, Afsharan H, Eskandani M, Charoudeh HN, Rashidi M-R (2016) Reduced graphene oxide decorated with gold nanoparticle as signal amplification element on ultra-sensitive electrochemiluminescence determination of caspase-3 activity and apoptosis using peptide based biosensor. BioImpacts: BI 6(3):135–147
23. Feng Q, Wang M, Zhao X, Wang P (2018) Construction of a cytosine-adjusted Electrochemiluminescence resonance energy transfer system for MicroRNA detection. Langmuir 34(34):10153–10162
24. Lin Y, Wang J, Luo F, Guo L, Qiu B, Lin Z (2018) Highly reproducible ratiometric aptasensor based on the ratio of amplified electrochemiluminescence signal and stable internal reference electrochemical signal. Electrochim Acta 283:798–805
25. Heidari R, Rashidiani J, Abkar M, Taheri RA, Moghaddam MM, Mirhosseini SA, Seidmoradi R, Nourani MR, Mahboobi M, Keihan AH (2019) CdS nanocrystals/graphene oxide-AuNPs based electrochemiluminescence immunosensor in sensitive quantification of a cancer biomarker: p53. Biosens Bioelectron 126:7–14
26. Jie G, Lu Z, Zhao Y, Wang X (2017) Quantum dots bilayers/au@Ag-based electrochemiluminescence resonance energy transfer for detection of thrombin by autocatalytic multiple amplification strategy. Sensors Actuators B Chem 240:857–862
27. Lin Z, Chen L, Zhu X, Qiu B, Chen G (2010) Signal-on electrochemiluminescence biosensor for thrombin based on target-induced conjunction of split aptamer fragments. Chem Commun 46(30):5563–5565
28. Zhuo B, Li Y, Huang X, Lin Y, Chen Y, Gao W (2015) An electrochemiluminescence aptasensing platform based on ferrocene-graphene nanosheets for simple and rapid detection of thrombin. Sensors Actuators B Chem 208:518–524
29. Liao Y, Yuan R, Chai Y, Mao L, Zhuo Y, Yuan Y, Bai L, Yuan S (2011) Electrochemiluminescence quenching via capture of

ferrocene-labeled ligand-bound aptamer molecular beacon for ultrasensitive detection of thrombin. Sensors Actuators B Chem 158(1):393–399
30. Zhang Y-Y, Zhou H, Wu P, Zhang H-R, Xu J-J, Chen H-Y (2014) In situ activation of CdS electrochemiluminescence film and its application in H2S detection. Anal Chem 86(17):8657–8664
31. Huang H, Zhu J-J (2009) DNA aptamer-based QDs electrochemiluminescence biosensor for the detection of thrombin. Biosens Bioelectron 25(4):927–930
32. Dhage SR, Colorado HA, Hahn HT (2013) Photoluminescence properties of thermally stable highly crystalline CdS nanoparticles. Mater Res 16(2):504–507
33. Liu J, Cao J, Li Z, Ji G, Deng S, Zheng M (2007) Low-temperature solid-state synthesis and phase-controlling studies of CdS nanoparticles. J Mater Sci 42(3):1054–1059
34. Shan Y, Xu J-J, Chen H-Y (2009) Distance-dependent quenching and enhancing of electrochemiluminescence from a CdS: Mn nanocrystal film by au nanoparticles for highly sensitive detection of DNA. Chem Commun 8:905–907
35. Yu H-X, Cui H (2005) Comparative studies on the electrochemiluminescence of the luminol system at a copper electrode and a gold electrode under different transient-state electrochemical techniques. J Electroanal Chem 580(1):1–8
36. Miao W (2008) Electrogenerated chemiluminescence and its biorelated applications. Chem Rev 108(7):2506–2553
37. Rashidiani J, Kamali M, Sedighian H, Akbariqomi M, Mansouri M, Kooshki H (2018) Ultrahigh sensitive enhanced-electrochemiluminescence detection of cancer biomarkers using silica NPs/graphene oxide: a comparative study. Biosens Bioelectron 102:226–233
38. Fang L, Lü Z, Wei H, Wang E (2008) A electrochemiluminescence aptasensor for detection of thrombin incorporating the capture aptamer labeled with gold nanoparticles immobilized onto the thio-silanized ITO electrode. Anal Chim Acta 628(1):80–86
39. Li F, Cui H (2013) A label-free electrochemiluminescence aptasensor for thrombin based on novel assembly strategy of oligonucleotide and luminol functionalized gold nanoparticles. Biosens Bioelectron 39(1):261–267
40. Shao K, Wang B, Ye S, Zuo Y, Wu L, Li Q, Lu Z, Tan X, Han H (2016) Signal-amplified near-infrared ratiometric electrochemiluminescence aptasensor based on multiple quenching and enhancement effect of graphene/gold nanorods/G-quadruplex. Anal Chem 88(16):8179–8187
41. Li Y, Li Y, Xu N, Pan J, Chen T, Chen Y, Gao W (2017) Dual-signal amplification strategy for electrochemiluminescence sandwich biosensor for detection of thrombin. Sensors Actuators B Chem 240: 742–748

**Publisher's note** Springer Nature remains neutral with regard to jurisdictional claims in published maps and institutional affiliations.